ACS Macro Letters

pubs.acs.org/macroletters Letter

Autonomous Construction of Phase Diagrams of Block Copolymers by Theory-Assisted Active Machine Learning

Shuochen Zhao, Tianyun Cai, Liangshun Zhang,* Weihua Li,* and Jiaping Lin*

Cite This: *ACS Macro Lett.* 2021, 10, 598−602 Read Online

ACCESS | Metrics & More | Article Recommendations | Supporting Information

ABSTRACT: Equilibrium phase diagrams serve as blueprints for rational design of nanostructured materials of block copolymers, but their construction is time-consuming and requires profound expertise. Herein, by virtue of the knowledge of self-consistent field theory (SCFT), the active-learning method is developed to autonomously construct the phase diagrams of block copolymers. Without human intervention, the SCFT-assisted active-learning method can rapidly search the undetected phases and efficiently reproduce the complicated phase diagrams of diblock copolymers and multiblock terpolymers via decreasing the number of sampling points to about 20%. It is clearly demonstrated that the combined uncertainty sampling/random selection scheme in the active-learning method shows the outperformance in spite of a small amount of initial data set. This work highlights the promising integration of theoretical modeling with machine learning and represents a crucial step toward rational design of nanostructured materials.

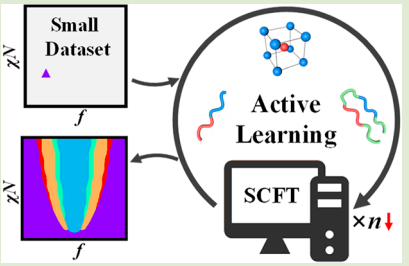

Driven by a compromise between the minimization of unfavorable contacts and the maximization of configurational entropy, block copolymers self-assemble into a diversity of ordered nanostructures or "nanophases", which can act as building units to develop next-generation devices as well as create functional metamaterials.[1−3] Equilibrium phase diagrams, which represent the dependence of thermodynamic phases on a suite of variables (e.g., compositions and interaction parameters), serve as blueprints for designing the structural and functional materials. Currently, the phase diagrams of diblock copolymers were mapped by grid search methods,[4−6] which require profound expertise and time/cost-intensive investigations. Beyond the diblock copolymers, incorporating distinct blocks and block types offers unlimited potentials for achievement of extraordinary nanostructures, but leads to a daunting challenge for the phase-diagram construction in an expansive parameter space.[7,8] Thus, an advanced paradigm without human-decision is highly desirable to construct the complicated phase diagrams through a reduction of laborious and costly task.

Recently, machine-learning methods have been of tremendous utility and growth in a variety of fields,[9−11] including the polymer science.[12−16] Training a surrogate model to predict the properties of molecules or materials often requires large quantities of labeled data, which are actually scarce due to the difficulties of high-throughput synthesis and automatic characterization of polymers. Starting with "a small dataset", an active-learning method (i.e., a verification-by-learning framework) augments the observations into the training data set on-the-fly, dramatically reducing the number of labeled data for the reliable surrogate model.[17−20] Especially, on the basis of the Gaussian process regression and the uncertainty sampling, the active-learning methods were, respectively, applied to accelerate the construction of phase diagrams of active matter and inorganic compounds.[21,22] However, considering the diversity and complexity of block copolymers, there are so far very few studies that use the active-learning method to make surrogate predictions for their phase diagrams. If available, such data-driven workflows could be extremely helpful in the rational design of nanostructured materials of block copolymers.

In this contribution, in conjunction with the well-developed SCFT,[23,24] the active-learning method is proposed to autonomously generate the training data of estimated phase diagrams on-the-fly and thereby reduces both the size of the training data and the computational intensity of SCFT for the phase diagrams. It is demonstrated that the SCFT-assisted active-learning method can efficiently train a high-quality surrogate model to construct the phase diagrams of block copolymers without human intervention. Furthermore, our proposed method is generalized to accelerate the autonomous construction of complicated phase diagrams of multiblock terpolymers. Note that the current active-learning method is most suitable for the studies, where the explored phases are already known, but the phase boundaries need to be explored.

Received: March 3, 2021
Accepted: April 23, 2021
Published: April 27, 2021

Figure 1 schematically illustrates the workflow of autonomous construction of phase diagrams through integration of

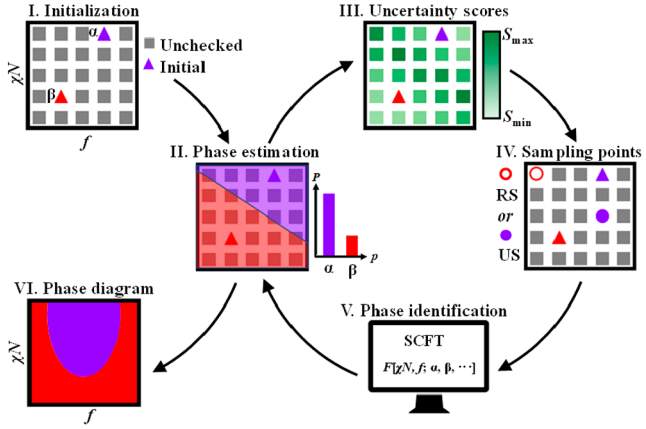

Figure 1. Closed-loop autonomous construction of phase diagrams based on physics-informed active learning.

active-learning method and theory-based knowledge. (I) A few initial points in the composition (f)−Flory−Huggins (χN) parameter space of phase diagrams are randomly selected and labeled by indices $p = [\alpha, \beta, ...]$ of equilibrium phases. (II) Label propagation algorithm is applied to deduce probability distributions $P(\mathbf{X}, p)$ of labeled phases p for all unchecked points at position $\mathbf{X}$ of parameter space.[25] (III) $P(\mathbf{X}, p)$ are used to calculate uncertainty scores $S(\mathbf{X})$ by the margin sampling estimator.[26] (IV) Next, the candidate point is recommended from unchecked points with the maximum uncertainty score if $S_{max} - S_{min} \geq \delta$, denoted by the uncertainty sampling (US) scheme, where S_{max}, S_{min}, and δ are, respectively, the maximum, minimum, and trade-off values of $S(\mathbf{X})$. In the case of $S_{max} - S_{min} < \delta$, a random selection (RS) scheme is introduced to recommend next candidate. (V) For the recommended candidate, the SCFT is used to identify the equilibrium phases. The above steps II−V are repeated until the phase diagrams are acceptably refined. (VI) Final phase diagrams with finer grid of parameter space are estimated by the method of phase estimation in step II. More details about the model can refer to Parts A and B of the Supporting Information (SI).

We first demonstrate that the SCFT-assisted active-learning method with a minimal amount of initial data set can autonomously construct the phase diagrams of simple AB diblock copolymers. Figures 2 and S1 of the SI show the refinement of phase diagrams of diblock copolymers. Considering the mirror symmetry indicated by the dashed lines in Figure 2, we only sample the left portion, but draw the full diagrams in the range of $0.1 \leq f \leq 0.9$ and $10.0 \leq \chi N \leq 20.0$, which are divided into 41×41 grid. A single point labeled by the disordered state (Dis) is used to warm up the training process of active learning. After 10 cycles of active learning, a variety of unlabeled phases (i.e., lamellae (Lam), hexagonally packed cylinders (Hex), body-centered-cubic spheres (BCC), and gyroid (Gyr)) are detected (Figure 2a). The phase diagrams are gradually refined as the cycles of active learning continue to be advanced (Figure S1 of the SI).

As shown in the left panel of Figure 2b, a total of 162 sampling points are mainly distributed around the phase boundaries, indicating the realization of efficient sampling of phase diagram. Right panel of Figure 2b shows the final phase

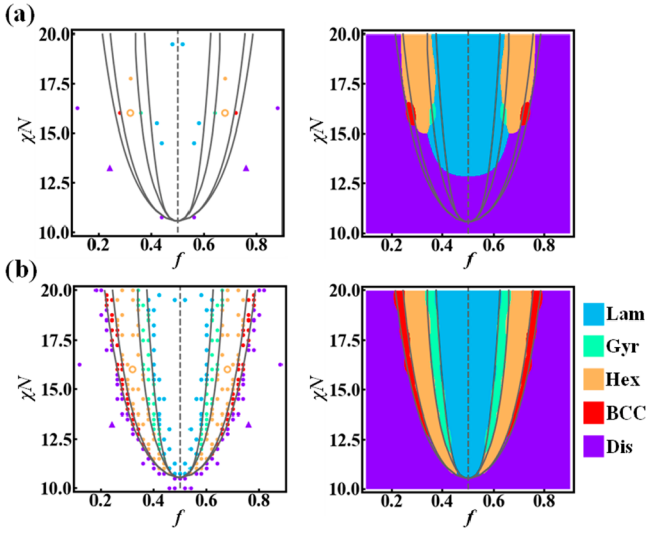

Figure 2. Refinement of f−χN phase diagrams of diblock copolymers via the US/RS scheme in the SCFT-assisted active learning. The set of diagrams is obtained after (a) $n_C = 10$ and (b) $n_C = 162$ cycles of active learning. (Left) Summarization of already sampling points. The triangles, filled and hollow circles represent the initial, uncertainty sampling and random selection points, respectively. (Right) Estimated phase diagrams by the active-learning method. The sampling points and phases' regions are represented by various colors. The solid lines represent the accurate phase boundaries.[27]

diagram of diblock copolymers under the 599×300 grid of parameter space. The accurate phase diagram is reproduced by the trained surrogate model of active-learning method. This example clearly demonstrates that our developed method is able to recommend the sampling points of phase diagram and to train a high-quality surrogate model for the reproduction of classic phase diagrams of diblock copolymers.

An important improvement of our developed method is that the uncertainty sampling is combined with the random selection to recommend the next candidates in the cycles of active learning. For comparison, we also present the results of random selection only (RS only) and uncertainty sampling only (US only). Since lots of candidates are randomly selected away from the phase boundaries, the efficient sampling is not realized for the RS only (Figure S2 of the SI). For the US only, the candidate points are intensively recommended in the lower f region (Figure S3 of the SI), which leads to a great difficulty in detecting all phases. Such issues can be resolved by the US/RS scheme, where the recommendation of sampling points is provided by the integration of effective decision-making route for next-best candidates and random fashion of gained knowledge. This integration allows us to rapidly search the undetected phases and intensively refine the boundaries of detected phases. Consequently, the RS/US scheme lowers the total computational intensity of SCFT due to a reduction of considered candidates (i.e., the number of cycles) for the phase diagrams.

Next, we introduce the number of detected phases and macro-averaged F1 (Macro-F1) score to quantitatively evaluate the performance of phase-diagram construction. Especially, Macro-F1 score assesses the accuracy of estimated phase diagrams.[28] For a phase indexed by p, F1 score is written as $F1(p) = 2Pr(p)Re(p)/(Pr(p) + Re(p))$, where $Pr(p)$ and $Re(p)$ are, respectively, the precision and the recall. The Macro-F1 score is defined as the arithmetic mean of F1 scores

https://doi.org/10.1021/acsmacrolett.1c00133
ACS Macro Lett. 2021, 10, 598−602

of all labeled phases. When the Macro-F1 score approaches one, the estimated phase diagram exactly reproduces the accurate one.

Figure 3a,b shows the number of detected phases and the Macro-F1 score as a function of the number n_C of cycles for

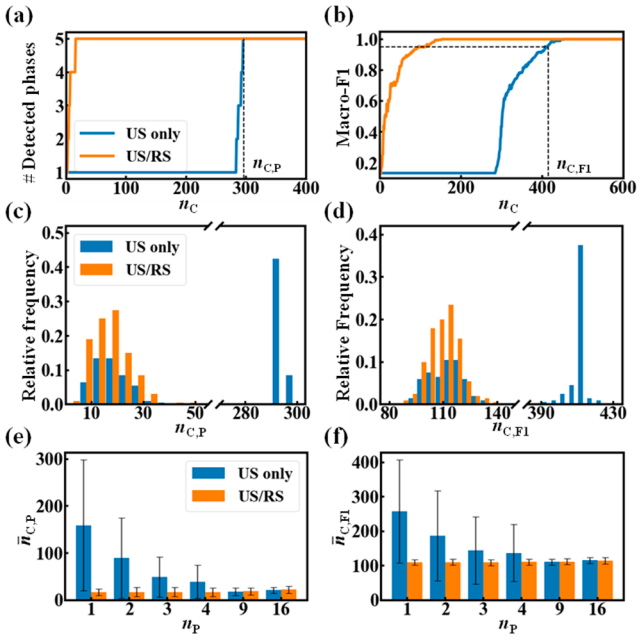

Figure 3. Performance comparison of phase-diagram construction via the US and US/RS schemes. (a) Number of detected phases and (b) Macro-F1 score as a function of the number n_C of cycles. The number of initial points is one. (c, d) Histograms of relative frequencies of $n_{C,P}$ and $n_{C,F1}$. (e, f) Average numbers $\bar{n}_{C,P}$ and $\bar{n}_{C,F1}$ as a function of the number n_P of initial points. The error bars stand for the standard deviations.

the US and US/RS schemes. About 300 cycles are required to detect all phases for the US scheme only. However, the US/RS scheme remarkably reduces the number of cycles to detect all phases, because it is able to search unexplored regions of phase diagrams by the random selection of candidate points. Correspondingly, the curves of Macro-F1 score have a sharp slope at this stage. After detecting all phases, the diagrams are mainly sampled around the phase boundaries, and the change rate of Macro-F1 score slows down. Eventually, the accuracy of estimated phase diagrams reaches the stopping criteria, that is, $1 - \text{Macro-F1} \leq 10^{-3}$. Therefore, the outperformance of US/RS scheme originates from the fact that the undetected phases can be rapidly searched by the RS scheme, accompanying the recommendation of "next-best candidates" in the US scheme.

In order to assess the effect of random choice of initial points, the entire workflow of active learning is repeated 200 times for each sampling scheme. Figure 3c,d shows the relative frequency distributions of the number $n_{C,P}$ of cycles to detect all phases and the number $n_{C,F1}$ of cycles to reach a Macro-F1 score of 0.95 (as defined in Figure 3a,b). As the active learning adopts the US/RS scheme, both histograms respectively exhibit narrow distributions with a single peak at $n_{C,P} = 20$ and $n_{C,F1} = 120$. However, for the US only, the frequency distributions shift to larger numbers of cycles and exist the bimodal population.

The average numbers of $n_{C,P}$ and $n_{C,F1}$ as well as their standard deviations are calculated to evaluate the performance of active learning in terms of the number n_P of initial points (Figure 3e,f). For both sampling schemes, the performance of active learning becomes excellent with an increase of n_P. However, in the case of $n_P \leq 4$, the US/RS scheme performs exceptionally well in comparison with the US scheme only. Particularly, it requires less cycles to detect all phases and reach a Macro-F1 score of 0.95. Meantime, the performance of US/RS scheme is weakly dependent upon the random choice of initial points (i.e., small standard deviations). These findings of Figure 3 manifest the fact that it is enough to utilize a small amount of initial data set to realize the outperformance of active learning via the US/RS scheme.

Furthermore, the performance of these sampling schemes is evaluated against the RS scheme only for $n_P = 1$ (Table 1). The

Table 1. Performance Comparison of Phase-Diagram Construction via the US/RS, US, and RS Schemes

sampling scheme	$\bar{n}_{C,P}$	$\bar{n}_{C,F1}$
US/RS	17 (0.61)[a]	110 (0.21)
US only	159 (5.68)	258 (0.49)
RS only	28 (1.00)	528 (1.00)

[a]The parentheses denote the reduction ratios of US/RS and US schemes in comparison with the RS scheme.

US/RS scheme rapidly finds all phases. The average number $\bar{n}_{C,F1}$ of cycles is reduced to ~20% through using the US/RS scheme, which still remains a high accuracy of estimated phase diagrams. Note that the estimator of uncertainty scores and the trade-off value δ also play important roles in affecting the performance of active learning (Figures S4−S7 of the SI).

Importantly, the active-learning method can be extended to reduce the SCFT calculations of possible phases and propose the conditions of unstudied phases. On the basis of the probability distributions P of labeled phases, the scheme of top candidates can reduce the computational intensity of possible phases to about 80% (Figure S8 of the SI). The scheme of entropy-based uncertainty scores defined in eq S11 of the SI is proposed to recommend the possible regions of novel phases (Figure S9 of the SI).

With these backgrounds in place, we finally shift our focus to a more challenging issue, demonstrating the generalization of autonomous construction for extremely complicated phase diagrams of block copolymers. As a typical example, linear $B_1AB_2CB_3$ pentablock terpolymers consist of the incompatibility A and C blocks (Figure 4a),[29,30] which respectively form distinct nanodomains connected by middle B_2 blocks. The multiblock terpolymers self-assemble into a broad spectrum of mesocrystals. Particularly, through tuning the composition f_A of A or C blocks and the composition f_{B2} of B_2 blocks, the pentablock terpolymers form binary spherical mesocrystals including CsCl with $Pm\bar{3}m$ symmetry, ZnS_C with $F\bar{4}3m$, NaCl with $Fm\bar{3}m$ and α-BN with $P6_3/mmc$, and cylindrical phases (e.g., hexagonally packed cylinders $C_{A/C}$, C^4_{P4mm}, C^3_{P3m1}, and C^2_{C2mm}, where the superscript indicates the coordination number), which are shown in Figure 4b. The diversity and complexity of the ordered nanostructures dramatically increase the difficulties of phase-diagram construction.

We herein concentrate on the two-dimensional, known phase diagram with respect to the f_A−f_{B2} parameter space under the restrictions of the composition $f_A = f_C$ and $f_{B1} = f_{B3}$, as well as the Flory−Huggins interaction parameters $\chi_{AB}N = \chi_{AC}N = \chi_{BC}N = 80.0$. Initially, a single point is randomly

https://doi.org/10.1021/acsmacrolett.1c00133
ACS Macro Lett. 2021, 10, 598−602

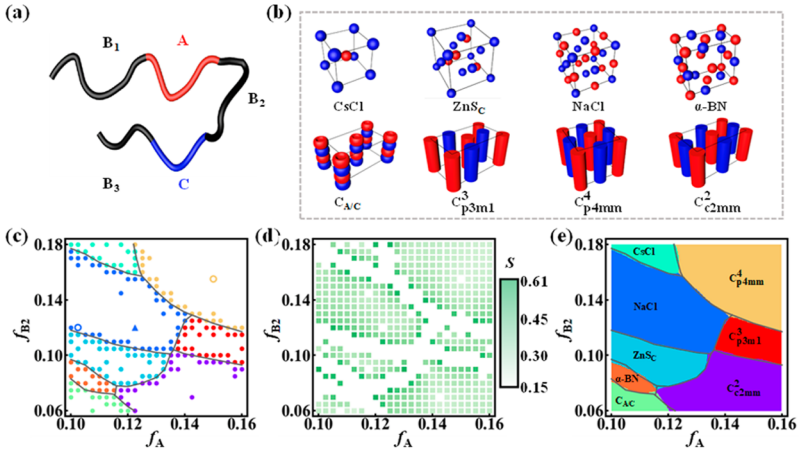

Figure 4. (a) Molecular architecture of $B_1AB_2CB_3$ pentablock terpolymers. (b) Ordered nanostructures of pentablock terpolymers. The A- and C-rich nanodomains are indicated by the red and blue colors, respectively. (c) Summarization of already sampling points in the active learning. (d) Plot of uncertainty scores. (e) Estimated phase diagram of active learning. The solid lines represent the original phase boundaries of SCFT.[29]

selected in the extremely narrow range of $0.10 \leq f_A \leq 0.16$ and $0.06 \leq f_{B2} \leq 0.18$, which are divided into 25×25 grid. Figure 4c–e shows the final refined results of active learning for the pentablock terpolymers. The 200 sampling points in the narrow f_A–f_{B2} parameter space are mainly distributed around the phase boundaries with higher uncertainty scores. The trained surrogate model of active learning correctly replicates the complicated phase diagram of pentablock terpolymers, and the estimated boundaries have a good match with the human-determined curves.[29] Therefore, the SCFT-assisted active-learning method can autonomously construct the complicated phase diagrams of multiblock terpolymers.

In summary, we develop an active-learning method in conjunction with the SCFT to successfully accelerate the autonomous construction of phase diagrams of block copolymers. It is demonstrated that our proposed US/RS scheme in the active-learning method shows the best performance in terms of the number of detected phases and the accuracy of estimated phase diagrams, in spite of a small amount of initial data set. Furthermore, the developed active-learning method could be applied to accelerate the autonomous construction of complicated phase diagrams of multiblock terpolymers. It should be mentioned that the avenue forward for the further improvement of active learning lies in the usages of multipoint sampling in each cycle and label propagation algorithm considering the free energy landscape.[21,25]

■ ASSOCIATED CONTENT

Supporting Information

The Supporting Information is available free of charge at https://pubs.acs.org/doi/10.1021/acsmacrolett.1c00133.

Self-consistent field theory of block copolymers; Phase diagram construction via active learning; Additional figures (PDF)

■ AUTHOR INFORMATION

Corresponding Authors

Liangshun Zhang − *Shanghai Key Laboratory of Advanced Polymeric Materials, Key Laboratory for Ultrafine Materials of Ministry of Education, School of Materials Science and Engineering, East China University of Science and Technology, Shanghai 200237, China;* orcid.org/0000-0002-0182-7486; Email: zhangls@ecust.edu.cn

Weihua Li − *State Key Laboratory of Molecular Engineering of Polymers, Key Laboratory of Computational Physical Sciences, Department of Macromolecular Science, Fudan University, Shanghai 200438, China;* orcid.org/0000-0002-5133-0267; Email: weihuali@fudan.edu.cn

Jiaping Lin − *Shanghai Key Laboratory of Advanced Polymeric Materials, Key Laboratory for Ultrafine Materials of Ministry of Education, School of Materials Science and Engineering, East China University of Science and Technology, Shanghai 200237, China;* orcid.org/0000-0001-9633-4483; Email: jlin@ecust.edu.cn

Authors

Shuochen Zhao − *Shanghai Key Laboratory of Advanced Polymeric Materials, Key Laboratory for Ultrafine Materials of Ministry of Education, School of Materials Science and Engineering, East China University of Science and Technology, Shanghai 200237, China*

Tianyun Cai − *Shanghai Key Laboratory of Advanced Polymeric Materials, Key Laboratory for Ultrafine Materials of Ministry of Education, School of Materials Science and Engineering, East China University of Science and Technology, Shanghai 200237, China*

Complete contact information is available at: https://pubs.acs.org/10.1021/acsmacrolett.1c00133

Notes

The authors declare no competing financial interest.

■ ACKNOWLEDGMENTS

This work was supported by the National Natural Science Foundation of China (22073028, 21873029, 51833003, and 21925301). We sincerely thank the anonymous reviewers for their helpful suggestions, which result in substantial improvements of the model.

■ REFERENCES

(1) Bates, F. S.; Fredrickson, G. H. Block Copolymer Thermodynamics: Theory and Experiment. *Annu. Rev. Phys. Chem.* **1990**, *41*, 525–557.

(2) Bates, C. M.; Maher, M. J.; Janes, D. W.; Ellison, C. J.; Willson, C. G. Block Copolymer Lithography. *Macromolecules* **2014**, *47*, 2−12.
(3) Hampu, N.; Werber, J. R.; Chan, W. Y.; Feinberg, E. C.; Hillmyer, M. A. Next-Generation Ultrafiltration Membranes Enabled by Block Polymers. *ACS Nano* **2020**, *14*, 16446−16471.
(4) Bates, F. S.; Schulz, M. F.; Khandpur, A. K.; Förster, S.; Rosedale, J. H.; Almdal, K.; Mortensen, K. Fluctuations, Conformational Asymmetry and Block Copolymer Phase Behaviour. *Faraday Discuss.* **1994**, *98*, 7−18.
(5) Lee, S.; Bluemle, M. J.; Bates, F. S. Discovery of a Frank- Kasper Phase in Sphere-Forming Block Copolymer Melts. *Science* **2010**, *330*, 349−353.
(6) Li, W.; Liu, M.; Qiu, F.; Shi, A.-C. Phase Diagram of Diblock Copolymers Confined in Thin Films. *J. Phys. Chem. B* **2013**, *117*, 5280−5288.
(7) Qin, J.; Bates, F. S.; Morse, D. C. Phase Behavior of Nonfrustrated ABC Triblock Copolymers: Weak and Intermediate Segregation. *Macromolecules* **2010**, *43*, 5128−5136.
(8) Bates, F. S.; Hillmyer, M. A.; Lodge, T. P.; Bates, C. M.; Delaney, K. T.; Fredrickson, G. H. Multiblock Polymers: Panacea or Pandora's Box? *Science* **2012**, *336*, 434−440.
(9) Butler, K. T.; Davies, D. W.; Cartwright, H.; Isayev, O.; Walsh, A. Machine Learning for Molecular and Materials Science. *Nature* **2018**, *559*, 547−555.
(10) Moosavi, S. M.; Jablonka, K. M.; Smit, B. The Role of Machine Learning in the Understanding and Design of Materials. *J. Am. Chem. Soc.* **2020**, *142*, 20273−20287.
(11) Batra, R.; Song, L.; Ramprasad, R. Emerging Materials Intelligence Ecosystems Propelled by Machine Learning. *Nat. Rev. Mater.* **2020**, na DOI: 10.1038/s41578-020-00255-y.
(12) Audus, D. J.; de Pablo, J. J. Polymer Informatics: Opportunities and Challenges. *ACS Macro Lett.* **2017**, *6*, 1078−1082.
(13) Aoyagi, T. Deep Learning Model for Predicting Phase Diagrams of Block Copolymers. *Comput. Mater. Sci.* **2021**, *188*, 110224.
(14) Tu, K.; Huang, H.; Lee, S.; Lee, W.; Sun, Z.; Alexander-Katz, A.; Ross, C. A. Machine Learning Predictions of Block Copolymer Self-Assembly. *Adv. Mater.* **2020**, *32*, 2005713.
(15) Khadilkar, M. R.; Paradiso, S. P.; Delaney, K. T.; Fredrickson, G. H. Inverse Design of Bulk Morphologies in Multiblock Polymers Using Particle Swarm Optimization. *Macromolecules* **2017**, *50*, 6702−6709.
(16) Li, J.; Zhang, H.; Chen, J. Z. Y. Structural Prediction and Inverse Design by a Strongly Correlated Neural Network. *Phys. Rev. Lett.* **2019**, *123*, 108002.
(17) Kim, C.; Chandrasekaran, A.; Jha, A.; Ramprasad, R. Active-Learning and Materials Design: The Example of High Glass Transition Temperature Polymers. *MRS Commun.* **2019**, *9*, 860−866.
(18) Loeffler, T. D.; Patra, T. K.; Chan, H.; Cherukara, M.; Sankaranarayanan, S. K. R. S. Active Learning the Potential Energy Landscape for Water Clusters from Sparse Training Data. *J. Phys. Chem. C* **2020**, *124*, 4907−4916.
(19) Tian, Y.; Yuan, R.; Xue, D.; Zhou, Y.; Ding, X.; Sun, J.; Lookman, T. Role of Uncertainty Estimation in Accelerating Materials Development *via* Active Learning. *J. Appl. Phys.* **2020**, *128*, 014103.
(20) Shmilovich, K.; Mansbach, R. A.; Sidky, H.; Dunne, O. E.; Panda, S. S.; Tovar, J. D.; Ferguson, A. L. Discovery of Self-Assembling π-Conjugated Peptides by Active Learning-Directed Coarse-Grained Molecular Simulation. *J. Phys. Chem. B* **2020**, *124*, 3873−3891.
(21) Dai, C.; Glotzer, S. C. Efficient Phase Diagram Sampling by Active Learning. *J. Phys. Chem. B* **2020**, *124*, 1275−1284.
(22) Terayama, K.; Tamura, R.; Nose, Y.; Hiramatsu, H.; Hosono, H.; Okuno, Y.; Tsuda, K. Efficient Construction Method for Phase Diagrams Using Uncertainty Sampling. *Phys. Rev. Mater.* **2019**, *3*, 033802.
(23) Matsen, M. W. The Standard Gaussian Model for Block Copolymer Melts. *J. Phys.: Condens. Matter* **2002**, *14*, R21−R47.
(24) Arora, A.; Qin, J.; Morse, D. C.; Delaney, K. T.; Fredrickson, G. H.; Bates, F. S.; Dorfman, K. D. Broadly Accessible Self-Consistent Field Theory for Block Polymer Materials Discovery. *Macromolecules* **2016**, *49*, 4675−4690.
(25) Zhu, X.; Ghahramani, Z.; Lafferty, J. Semi-Supervised Learning Using Gaussian Fields and Harmonic Functions. *Proceedings of the Twentieth International Conference on Machine Learning*; AAAI Press, 2003; 912−919.
(26) Scheffer, T.; Decomain, C.; Wrobel, S. Active Hidden Markov Models for Information Extraction. *In Lecture Notes in Computer Science (including subseries Lecture Notes in Artificial Intelligence and Lecture Notes in Bioinformatics)*; **2001**, *2189*, 309−318.
(27) Matsen, M. W.; Bates, F. S. Unifying Weak- and Strong-Segregation Block Copolymer Theories. *Macromolecules* **1996**, *29*, 1091−1098.
(28) Yang, Y. An Evaluation of Statistical Approaches to Text Categorization. *Inf. Retr. Boston.* **1999**, *1*, 69−90.
(29) Xie, N.; Liu, M.; Deng, H.; Li, W.; Qiu, F.; Shi, A.-C. Macromolecular Metallurgy of Binary Mesocrystals *via* Designed Multiblock Terpolymers. *J. Am. Chem. Soc.* **2014**, *136*, 2974−2977.
(30) Xie, Q.; Qiang, Y.; Li, W. Regulate the Stability of Gyroids of ABC-Type Multiblock Copolymers by Controlling the Packing Frustration. *ACS Macro Lett.* **2020**, *9*, 278−283.

https://doi.org/10.1021/acsmacrolett.1c00133
ACS Macro Lett. 2021, 10, 598−602